AJNR

Clinical Usefulness of Unsubtracted 3D Digital Angiography Compared with Rotational Digital Angiography in the Pretreatment Evaluation of Intracranial Aneurysms

Toshinori Hirai, Yukunori Korogi, Kenji Suginohara, Ken Ono, Tomohiro Nishi, Shozaburo Uemura, Masayuki Yamura and Yasuyuki Yamashita

AJNR Am J Neuroradiol 2003, 24 (6) 1067-1074
http://www.ajnr.org/content/24/6/1067

AJNR Am J Neuroradiol 24:1067–1074, June/July 2003

Clinical Usefulness of Unsubtracted 3D Digital Angiography Compared with Rotational Digital Angiography in the Pretreatment Evaluation of Intracranial Aneurysms

Toshinori Hirai, Yukunori Korogi, Kenji Suginohara, Ken Ono, Tomohiro Nishi, Shozaburo Uemura, Masayuki Yamura, and Yasuyuki Yamashita

BACKGROUND AND PURPOSE: **Three-dimensional digital subtraction angiography (DSA) is useful as a supplement to 2D DSA in the pretreatment evaluation of intracranial aneurysms. However, the clinical efficacy of 3D digital angiography (DA) that is generated from unsubtracted rotational images has not been established. The purpose of this study was to assess whether 3D DA provides additional useful information to that of rotational DA in the preoperative evaluation of intracranial aneurysms.**

METHODS: **This prospective study comprised 23 patients (age range, 37–83 years) with ruptured aneurysms who underwent angiography. Two radiologists independently evaluated the rotational DA images and the maximum intensity projection, shaded surface display, and volume-rendering 3D DA images, in combination with 2D DSA images. A four-point scoring system was used to evaluate aneurysm detection and delineation. Referring neurosurgeons were questioned as to whether the information obtained with 3D DA was useful for treatment decisions.**

RESULTS: **Thirty aneurysms were confirmed by surgery or endovascular treatment. In detection and delineation of the 30 confirmed aneurysms, overall mean scores were highest with volume-rendering 3D DA and lowest with rotational DA. Compared with rotational DA, volume-rendering 3D DA demonstrated 27 additional findings in 14 (47%) of 30 aneurysms: detection of an aneurysm (n = 2), and delineation of aneurysm neck, shape, and relationship to adjacent arteries (n = 25). The information provided by 3D DA was useful for following treatment in five (22%) of 23 patients.**

CONCLUSION: **In the preoperative evaluation of intracranial aneurysms, 3D DA can provide additional useful information to that of rotational DA.**

Three-dimensional digital subtraction angiography (DSA) is useful as a supplement to 2D DSA in the pretreatment evaluation of intracranial aneurysms (1–5). Recently, 3D digital angiography (DA) was developed and has been applied clinically (6, 7). Three-dimensional DA images are generated from unsubtracted rotational images. The 3D DA technique has several theoretic advantages over 3D DSA: no chance of misregistration artifacts associated with the subtraction technique, less chance of motion artifacts by single acquisition, and lower radiation dose to patients. This technique may have possible disadvantages such as an inferior image quality to that of 3D DSA caused by unsubtracted image data. To our knowledge, however, no systematic studies have evaluated the usefulness of the 3D DA technique for pretreatment assessment of intracranial aneurysms. The purpose of this study was to assess whether 3D DA provides additional useful information to that of rotational DA in the pretreatment evaluation of intracranial aneurysms.

Received September 13, 2002; accepted after revision December 29, 2002.

From the Departments of Radiology (T.H., K.O., T.N.) and Neurosurgery (K.S., S.U.), Amakusa Medical Center, Kumamato, Japan, and the Department of Radiology, Kumamoto University School of Medicine, Japan (Y.K., M.Y., Y.Y.).

Address reprint requests to Toshinori Hirai, Department of Radiology, Amakusa Medical Center, 854–1 Kameba, Hondo, Kumamoto 863-0046 Japan.

Methods

Patients

Between August 2000 and August 2001, 34 consecutive patients with intracranial aneurysms prospectively underwent intraarterial 2D DSA, rotational DA, and 3D DA with an Integris BV 5000 angiographic biplane system (Philips Medical

Systems, Best, the Netherlands). Inclusion criteria for enrollment in this study were patients who underwent surgery or endovascular treatment after the angiographic evaluation. Seven patients did not undergo surgery or endovascular treatment because of small unruptured aneurysms (n = 3), difficulty in aneurysm treatment (n = 2), fusiform aneurysms (n = 1), or older age (n = 1). Four patients who had undergone endovascular coil embolization or surgical clipping before the angiographic evaluation were not included in this study. Therefore, the study population comprised 23 patients (17 women, six men; age range, 37–83 years; mean age, 64.1 years). Written informed consent was obtained from patients or their relatives. All the patients enrolled had a subarachnoid hemorrhage. The angiographic examination was performed the day the subarachnoid hemorrhage occurred (day 0) in 10 patients, within 1–3 days in nine patients, and at 4–10 days in four patients.

The 2D DSA Acquisition

Intraarterial DSA was performed with a 1024 × 1024 matrix. All catheterizations were performed by means of a transfemoral approach with the Seldinger technique. The angiographic procedure was accomplished with a standard diagnostic catheter. Selective three- or four-vessel angiography was performed in the anteroposterior and lateral projections. Since the 3D angiograms allow observation and analysis of an aneurysm from multiple views, we used limited two or three projections of 2D DSA when 3D DA with unsubtracted rotational images would be performed for a selected vessel that had an aneurysm or a suspected aneurysm. In patients with an anterior communicating aneurysm, DSA with manual compression of the contralateral carotid artery was performed to obtain more detailed information about the relationship between the aneurysm and the parent artery. Six images were selected for each projection and printed on hard-copy films.

The 3D DA Acquisition and Display

After 2D DSA studies were performed, rotational DA was performed with a field of view of 17 × 17 cm, by using the frontal plane of a biplanar C-arm. The counterbalanced, ceiling-suspended C-arm rotates in a continuous 180° (−90° to +90°) arc with the path of the x-ray tube. The isocenter for the rotational field was the area of interest in the patient's head. One hundred twenty digital angiograms with a 512 × 512 matrix were obtained with the 180° C-arm sweep, which rotates at a speed of 30°/s. The total 180° rotation was accomplished in 8 seconds. Mask images were not obtained.

A total of 24–32 mL of iopamidol (Iopamiron 300; Schering, Osaka, Japan) was injected into the internal carotid or vertebral artery at a flow rate of 3.0–4.0 mL/s by using a power injector (Auto Enhance A-50; Nemoto Kyorindo, Tokyo, Japan). The injection started 2.0 seconds before the acquisition of the first opacified image to provide entire filling of the selected arteries during rotational DA.

The unsubtracted rotational DA images were transferred to a workstation (3D-RA; Philips Medical Systems) for generating 3D DA images. A 128 × 128 × 128 3D angiogram that shows all the vessels included in the field of view is automatically displayed within 5 minutes after transfering all images to the 3D workstation. The 256 × 256 × 256 angiograms were generated after regions of interest were selected. Then, the aneurysm and parent artery were also reconstructed with a multiplanar reconstruction technique. We measured the diameter of each cerebral aneurysm with multiplanar reconstructions on the workstation. The maximum diameter of each aneurysm was classified as large (> 12 mm), medium (5–12 mm), small (3–4 mm), or very small (< 3 mm).

Display of the 3D DA images comprised three methods: maximum intensity projection (MIP), shaded surface display (SSD), and volume rendering. The reviewer determined the threshold of the vessels in each case by interactively observing the angiograms on the workstation. When demonstration of the small vessels or perforators in the region of interest was required, the threshold could be changed according to their visibility.

Assessment of Angiograms

Direct visualization of the aneurysm at surgery was used as the reference standard. Confirmation by means of endovascular treatment was also used as a reference standard for aneurysm detection. However, the aneurysms that underwent endovascular treatment were not used as the reference standard for aneurysm delineation because direct confirmation was not obtained.

With regard to the aneurysm detection and delineation, two radiologists (T.H., K.O.) independently reviewed four different display forms: rotational DA images and MIP, SSD, and volume-rendering 3D DA images. Additional information of 3D DA to that of rotational DA was also assessed for each aneurysm. The rotational DA and 3D DA images were always analyzed in conjunction with the corresponding 2D DSA images. The 2D DSA images were reviewed on hard-copy films, the rotational DA images were reviewed on a display monitor, and the 3D DA images were reviewed on a workstation. The final agreement was obtained by consensus. The following four-point scoring system was used to evaluate aneurysm detection (defined as the presence or absence of aneurysms) and delineation (defined as ease of visualization of aneurysm neck, shape, and location): +2, sufficient visualization; +1, ambiguous visualization; 0, poor visualization; −1, misinterpretation. Shape indicated the aneurysm contour, which included the number of lobes of the aneurysm. Neck meant the size of the aneurysm neck: narrow (smaller than the aneurysm diameter), medium (equal to the aneurysm diameter), or wide (larger than the aneurysm diameter). Location referred to the relationship between the aneurysm and adjacent arteries. The adjacent arteries included the anterior, middle, and posterior cerebral arteries; anterior and posterior communicating arteries; anterior choroidal artery; and basilar artery and its branches.

Neurosurgeons (S.U., K.S.) who performed or assisted at treatment were questioned as to whether the information provided by 3D DA was useful for treatment decisions. The contribution of 3D DA to treatment for each aneurysm was graded as follows: grade 2, provided further information that was helpful for surgical or endovascular treatment; grade 1, provided further information, but not helpful for surgery or endovascular treatment; or grade 0, provided no further information. When the neurosurgeons' answers were scored as grade 2, the neurosurgerons indicated how the information provided with 3D DA was helpful for following treatment.

Statistical Analyses

The κ statistic was used to assess interobserver reliability of each angiogram for the scoring of detection and delineation (8). The κ values greater than 0 were considered to indicate positive agreement; less than 0.4, positive but poor agreement; 0.41–0.75, good agreement; and greater than 0.75, excellent agreement (8). The mean values of the four-point scoring criteria among the rotational, MIP, SSD, and volume-rendering angiograms were tested with the Kruskal-Wallis test for multiple comparisons. Once a statistically significant difference was identified among the four angiogram groups, the Scheffe test was performed for comparisons of every pair of the groups. A P value of less than 0.05 was considered to indicate a statistically significant difference.

Results

In all patients, the angiographic procedures were successfully performed without any complications. A total of 30 aneurysms in the 23 patients were con-

TABLE 1: Aneurysm detection at rotational DA and MIP, SSD, and volume-rendering 3D DA

Aneurysm Detection Score*	Rotational DA (n = 30)	MIP 3D DA (n = 30)	SSD 3D DA (n = 30)	Volume-Rendering 3D DA (n = 30)
+2	24 (80)	25 (83)	27 (90)	29 (97)
+1	4 (13)	3 (10)	3 (10)	1 (3)
0	2 (7)	2 (7)	0 (0)	0 (0)
−1	0 (0)	0 (0)	0 (0)	0 (0)
Mean score ± SD	1.73 ± 0.58	1.77 ± 0.57	1.90 ± 0.31	1.97 ± 0.18

Note.—Data are number of aneurysms. Numbers in parentheses are percentages.

* +2 indicates sufficient visualization; +1, ambiguous visualization; 0, poor visualization; −1, misinterpretation.

firmed by surgery or endovascular treatment: very small aneurysms in three, small in five, medium in 20, and large in two. The aneurysms were located at the anterior cerebral artery (n = 12), middle cerebral artery (n = 12), internal carotid artery (n = 4), and basilar artery (n = 2). Surgical treatment was performed in 28 aneurysms of 21 patients, and transcatheter arterial embolization was performed with Guglielmi electrodetachable coils in two aneurysms of two patients. Surgical treatments consisted of clipping in 25 aneuryms, wrapping in two, and coating in one.

Aneurysm Detection

With regard to aneurysm detection, results of the final consensus review by two radiologists are summarized in Table 1. In the overall mean scores for each technique, rotational DA scored lower than MIP, SSD, and volume-rendering 3D DA. Volume-rendering 3D DA had the highest scores and enabled sufficient detection in all aneurysms except one, which was a very small aneurysm (1.5 mm) at the A1 portion of the anterior cerebral artery, evaluated as ambiguous visualization (Fig 1). In the multiple comparisons regarding the mean values of the four-point scoring, no statistically significant difference was found among the four angiogram groups ($P = .19$). The κ values for interrater variability between observers showed good agreement (rotational DA, 0.61; MIP, 0.65; SSD, 0.65; and volume-rendering DA, 0.72).

Aneurysm Delineation

The results of delineation regarding the 28 aneurysms that were confirmed by surgery are shown in Tables 2-4. In the evaluation of aneurysm neck with DA, the overall mean scores were highest with the volume-rendering 3D images and lowest with the rotational images (Table 2). The SSD 3D images score was somewhat lower for delineation of the aneurysm neck compared with MIP and volume-rendering 3D DA scores. Four of eight aneurysms evaluated as wide neck on SSD 3D images were interpreted as a medium neck on volume-rendering 3D images (Fig 1). With regard to mean values of four-point scoring, a statistically significant difference was found in the multiple comparisons ($P = .013$). The mean score for volume-rendering 3D DA was significantly higher than that for rotational DA ($P = .048$). However, no statistically significant differences were noted in the other pairs. The κ values for interobserver variability showed good agreement (rotational DA 0.57; MIP, 0.59; SSD, 0.65; and volume-rendering DA, 0.68).

With regard to aneurysm shape, rotational DA and MIP DA scores were lower than the SSD and volume-rendering 3D DA scores (Table 3). In the multiple comparisons, a statistically significant difference was found among the four angiogram groups ($P = .001$). Statistically significant differences were noted between rotational DA and SSD 3D DA ($P = .049$), between rotational DA and volume-rendering 3D DA ($P = .007$), and between MIP and volume-rendering 3D DA ($P = .027$). In the remaining pairs, no statistically significant differences were noted. The κ values for interrater variability between observers showed good agreement (rotational DA, 0.61; MIP, 0.65; SSD, 0.65; and volume-rendering DA, 0.68).

In the evaluation of aneurysm location, the overall mean scores were lowest with rotational DA (Table 4). With the evaluation of the MIP, SSD, and volume-rendering 3D DA, the sufficient visualization was markedly increased to 21 (75%), 26 (93%), and 27 (96%), respectively. With regard to mean scores of the four-point scoring, a statistically significant difference was found among the four angiogram groups in the multiple comparisons ($P = .001$). Statistically significant differences were noted between rotational DA and MIP 3D DA ($P = .004$), between rotational DA and SSD 3D DA ($P < .001$), and between rotational DA and volume-rendering 3D DA ($P < .001$). However, no statistically significant differences were noted between MIP and SSD 3D DA ($P = .469$), between MIP and volume-rendering 3D DA ($P = .33$), and between SSD and volume-rendering 3D DA ($P = .995$). The κ values for interrater variability between observers showed good agreement (rotational DA, 0.68; MIP, 0.71; SSD, 0.71; and volume-rendering DA, 0.74).

Additional Information Obtained with 3D DA

Compared with rotational DA, volume-rendering 3D DA demonstrated 27 additional findings in 14 (47%) of 30 aneurysms: detection of an aneurysm (n = 2) and delineation of aneurysm neck, shape, and relationship to adjacent arteries (n = 25) (Table 5). The information provided by 3D DA was ranked as grade 2 in five (22%) of 23 patients (Table 5). The reasons for grade 2 were as follows: valuable infor-

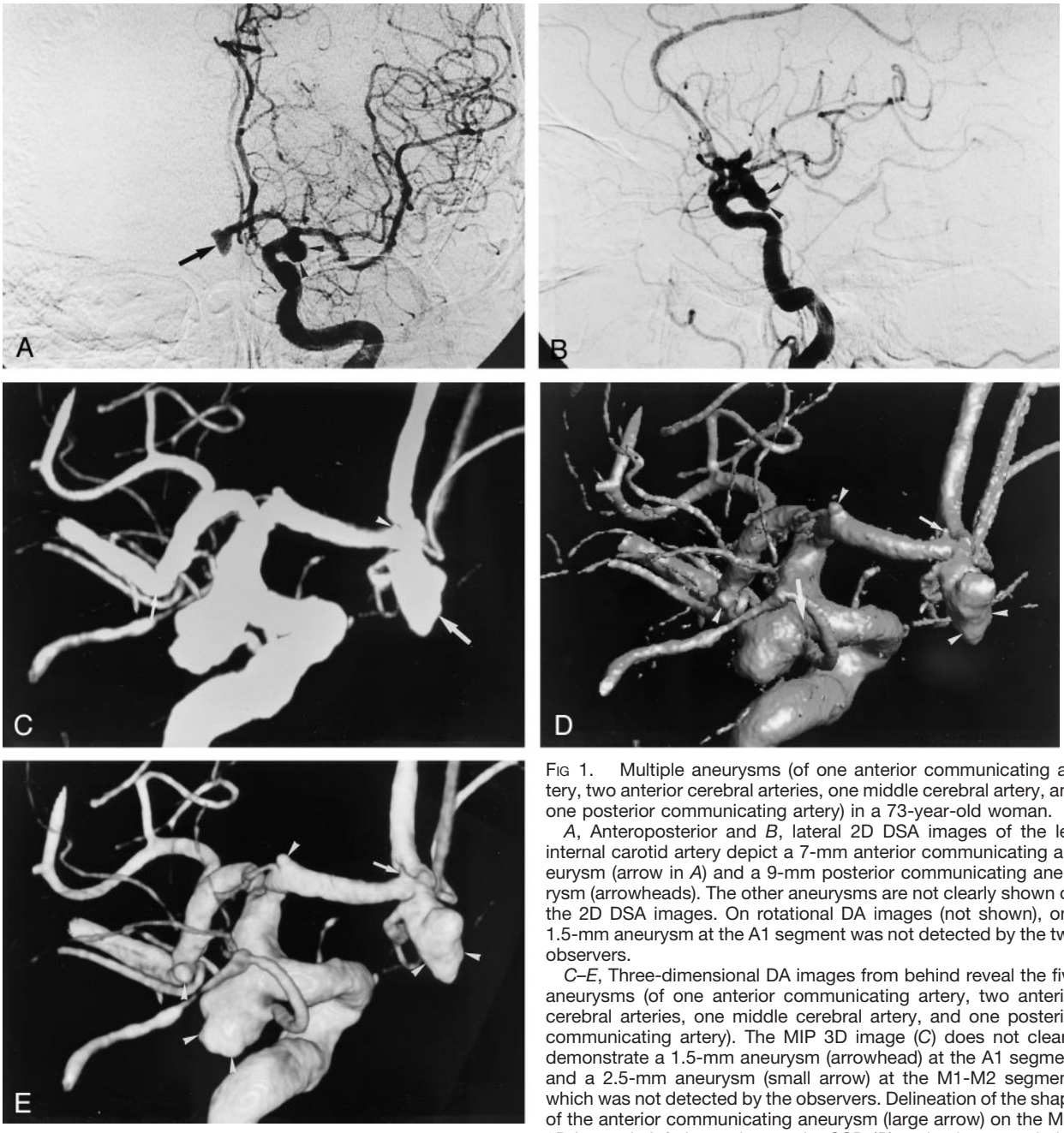

FIG 1. Multiple aneurysms (of one anterior communicating artery, two anterior cerebral arteries, one middle cerebral artery, and one posterior communicating artery) in a 73-year-old woman.

A, Anteroposterior and *B*, lateral 2D DSA images of the left internal carotid artery depict a 7-mm anterior communicating aneurysm (arrow in *A*) and a 9-mm posterior communicating aneurysm (arrowheads). The other aneurysms are not clearly shown on the 2D DSA images. On rotational DA images (not shown), one 1.5-mm aneurysm at the A1 segment was not detected by the two observers.

C–E, Three-dimensional DA images from behind reveal the five aneurysms (of one anterior communicating artery, two anterior cerebral arteries, one middle cerebral artery, and one posterior communicating artery). The MIP 3D image (*C*) does not clearly demonstrate a 1.5-mm aneurysm (arrowhead) at the A1 segment and a 2.5-mm aneurysm (small arrow) at the M1-M2 segment, which was not detected by the observers. Delineation of the shape of the anterior communicating aneurysm (large arrow) on the MIP 3D image is inferior to that on the SSD (*D*) and volume-rendering (*E*) 3D images because of lack of depth. On the SSD 3D image, the neck size of the posterior communicating aneurysm (large arrow in *D*) is overestimated compared with that on the volume-rendering 3D image (*E*). It is not clear whether the very small aneurysm (small arrow in *D*) at the A1 segment is an aneurysm or not. The two observers ranked it as ambiguous visualization. The other three aneurysms (arrowheads) are clearly demonstrated. On the volume-rendering image, the four aneurysms (arrowheads in *E*) were classified as sufficient visualization. However, the very small aneurysm (arrow in *E*) at the A1 segment was evaluated as ambiguous visualization. All the aneurysms were proved at surgery.

mation about whether treatment can be performed (n = 2) (Fig 2); critical information about what treatment should be chosen when treatment can be performed (n = 3) (Fig 2); and helpful information about manipulations of the aneurysm and adjacent arteries during surgery or endovascular treatment (n = 2) (Fig 1).

Two very small aneurysms at the A1 segment were detected only with 3D DA (Fig 1). In one anterior communicating aneurysm and one middle cerebral aneurysm with complicated vessels, 3D DA provided valuable and helpful information about manipulations of the aneurysm and adjacent arteries during surgery. In one large aneurysm at the distal anterior cerebral artery, the relationship between the aneurysm and the adjacent arteries was clearly demonstrated with SSD and volume-rendering 3D images (Fig 2). According to this finding, neurosurgeons made a decision to operate. In one medium aneurysm involving the posterior communicating artery and in-

TABLE 2: Delineation of aneurysm neck at rotational DA and MIP, SSD, and volume-rendering 3D DA

Delineation of Neck Score*	Rotational DA (n = 28)	MIP 3D DA (n = 28)	SSD 3D DA (n = 28)	Volume-Rendering 3D DA (n = 28)
+2	17 (61)	23 (82)	21 (75)	27 (96)
+1	7 (25)	3 (10)	4 (14)	1 (4)
0	4 (14)	1 (4)	2 (7)	0 (0)
−1	0 (0)	1 (4)	1 (4)	0 (0)
Mean score ± SD	1.46 ± 0.74	1.71 ± 0.71	1.61 ± 0.79	1.96 ± 0.19

Note.—Data are number of aneurysms. Numbers in parentheses are percentages.
* +2 indicates sufficient visualization; +1, ambiguous visualization; 0, poor visualization; −1, misinterpretation.

TABLE 3: Delineation of aneurysm shape at rotational DA and MIP, SSD, and volume-rendering 3D DA

Delineation of Shape Score*	Rotational DA (n = 28)	MIP 3D DA (n = 28)	SSD 3D DA (n = 28)	Volume-Rendering 3D DA (n = 28)
+2	16 (57)	18 (64)	24 (86)	27 (96)
+1	8 (29)	6 (21)	4 (14)	1 (4)
0	4 (14)	4 (14)	0 (0)	0 (0)
−1	0 (0)	0 (0)	0 (0)	0 (0)
Mean score ± SD	1.43 ± 0.74	1.50 ± 0.75	1.86 ± 0.36	1.96 ± 0.19

Note.—Data are number of aneurysms. Numbers in parentheses are percentages.
* +2 indicates sufficient visualization; +1, ambiguous visualization; 0, poor visualization; −1, misinterpretation.

TABLE 4: Delineation of relationship between aneurysm and adjacent arteries at rotational DA and MIP, SSD, and volume-rendering 3D DA

Delineation of Location Score*	Rotational DA (n = 28)	MIP 3D DA (n = 28)	SSD 3D DA (n = 28)	Volume-Rendering 3D DA (n = 28)
+2	12 (43)	21 (75)	26 (93)	27 (96)
+1	10 (36)	6 (21)	2 (7)	1 (4)
0	6 (21)	1 (4)	0 (0)	0 (0)
−1	0 (0)	0 (0)	0 (0)	0 (0)
Mean score ± SD	1.21 ± 0.79	1.71 ± 0.54	1.93 ± 0.26	1.96 ± 0.19

Note.—Data are number of aneurysms. Numbers in parentheses are percentages.
* +2 indicates sufficient visualization; +1, ambiguous visualization; 0, poor visualization; −1, misinterpretation.

ternal carotid artery, neurosurgeons decided on coating of the aneurysm dome based on 3D DA findings. The 3D DA images provided useful information about the neck and relationship to adjacent arteries in deciding on Guglielmi electrodetachable coil embolization in one basilar–superior cerebellar artery aneurysm.

Discussion

Rotational angiography complements the 2D angiographic method and improves the analysis of aneurysms compared with conventional angiography or 2D DSA (9–11). In complex aneurysms, however, precisely depicting aneurysm morphology may still be difficult. Three-dimensional DSA has been applied to the evaluation of intracranial aneurysms (1–5). The clinical results of the studies showed a definite superiority of 3D DSA over 2D DSA. Anxionnat et al (5) also demonstrated a superiority of 3D DSA over rotational DSA. Similar to their findings, our results showed a superiority of 3D DA over rotational DA. In rotational angiography, the views are in only a single plane of rotation and do not allow any cranial or caudal projections. A mental 3D reconstruction of the aneurysm is necessary for reviewing rotational angiograms. The limitations of rotational angiography do not allow objective understanding of the aneurysm morphology in complex cases.

Three-dimensional DA with unsubtracted rotational images has some theoretic advantages compared with 3D DSA. Although the 3D DSA technique requires contrast material–opacified images and mask images to obtain a subtraction imaging dataset, 3D DA does not need mask images. In this regard, beneficial effects are considered as follows. First, 3D DA may improve the image quality because there is no chance of misregistration associated with the subtraction technique. Second, 3D DA has less chance of motion artifacts than does 3D DSA. The acquisition of 3D DA is once, whereas 3D DSA is twice. Therefore, there is less probability of motion artifacts for 3D DA. Further investigation must be performed to determine whether 3D DA has better image quality than that of 3D DSA in the evaluation of intracranial aneurysms. Third, 3D DA is beneficial in reducing radiation dose to patients compared with 3D DSA. The radiation dose for mask images is not necessary for 3D DA.

Some authors have reported the clinical usefulness of 3D DSA with MIP and SSD (4, 5). However, all structures on MIP images are superimposed as 2D projection angiograms. This is due to the lack of

TABLE 5: Summary of additional information of 3D DA to that of rotational DA

Aneurysm No.	Site	Size (mm)	Treatment	Additional Information	Grade*
1	A1	4.7	Clip		0
2	A1	2	Wrap	Aneurysm detection	1
3	A1	1.5	Wrap	Aneurysm detection	1
4	A-com	10	Clip	Delineation of neck, shape, and location	2(c)
5	A-com	8	Clip	Delineation of neck and location	1
6	A-com	7	Clip	Delineation of location	1
7	A-com	7	Clip		0
8	A-com	6	Clip	Delineation of neck, shape, and location	1
9	A-com	6	Clip		0
10	A-com	5	Clip		0
11	Distal ACA	19	Clip	Delineation of location	2(a,b)
12	Distal ACA	9	Clip		0
13	IC-PC	10	Coat	Delineation of neck, shape, and location	2(a,b)
14	IC-PC	9	Clip	Delineation of neck and location	1
15	IC-PC	8	Clip		0
16	IC-PC	3.5	Clip		0
17	M1–M2	18	Clip	Delineation of neck	1
18	M1–M2	12	Clip	Delineation of location	1
19	M1–M2	10	Clip	Delineation of neck, shape, and location	2(c)
20	M1–M2	7	Clip		0
21	M1–M2	6	Clip		0
22	M1–M2	6	Clip	Delineation of neck and location	1
23	M1–M2	5	Clip		0
24	M1–M2	4	Clip		0
25	M1–M2	3.6	Clip		0
26	M1–M2	3	Clip		0
27	M1–M2	2.5	Clip		0
28	M1–M2	4	Clip		0
29	BA top	6	Coil		0
30	BA-SCA	5	Coil	Delineation of neck, shape, and location	2(b)

Note.—A1 indicates A1 segment of the anterior cerebral artery; A-com, anterior communicating artery; ACA, the anterior cerebral artery; IC-PC, internal carotid-posterior communicating artery; M1–M2, M1–M2 segment of the middle cerebral artery; BA, basilar artery; BA-SCA, basilar-superior cerebellar artery; clip, clipping; wrap, wrapping; coil, coil embolization.

* Grade 2, provided further information that was helpful for surgery or embolization; grade 1, provided further information, but not helpful for surgery or embolization; grade 0, provided no further information. Reasons affecting treatment: (a) valuable information about whether treatment can be performed; (b) critical information about what treatment should be chosen when treatment can be performed; and (c) helpful information about manipulations of the aneurysm and adjacent arteries during surgery or endovascular treatment.

depth of the vessels by MIP. Then, SSD may lead to a slight overestimation of the aneurysm and vessel size. Anxionnat et al (5) recommend simultaneous display of both MIP and SSD views because the two display methods complement each other. In our study, among the three 3D display techniques, volume rendering was the best mode of display to precisely visualize aneurysm morphology. Three-dimensional images with volume rendering have a number of theoretic advantages over MIP and SSD images (12, 13). The volume-rendered images maintain the original anatomic spatial relationships of the 3D angiographic data set and have a 3D appearance, facilitating interpretation of vascular interrelationships, which is limited with MIP images (13). Relative voxel attenuation is conveyed by means of a gray scale in the final image, which yields images that are more accurate than those rendered with SSD (13). The qualities of volume-rendered 3D angiography are essential for imaging the intracranial vasculature, especially vascular lesions such as aneurysms. Although the volume-rendering technique has computer constraints, the computer processing and display system used did not limit its practical and versatile use.

Very small aneurysms or aneurysms at complex sites can be missed with initial conventional angiography or DSA and may be found on a second arteriogram or during surgery (14). Since recognition of the location of the vessel wall, such as anterior, posterior, and lateral walls, can be easily obtained with SSD and volume-rendered 3D DA images, these images seem to be suitable for assessing aneurysms with the above conditions. In our study, we used several techniques to obtain high-quality images: the volume-rendering method for 3D reformation, a 512×512 matrix, and a selected field of view. These advantageous techniques probably contributed to the improved visualization of these aneurysms.

In this study, the additional information of 3D DA was useful for following treatment in some complicated or large aneurysms. Since the 3D angiograms allow the observation of an aneurysm from multiple views, better understanding about the relationship between the aneurysm and the adjacent arteries can

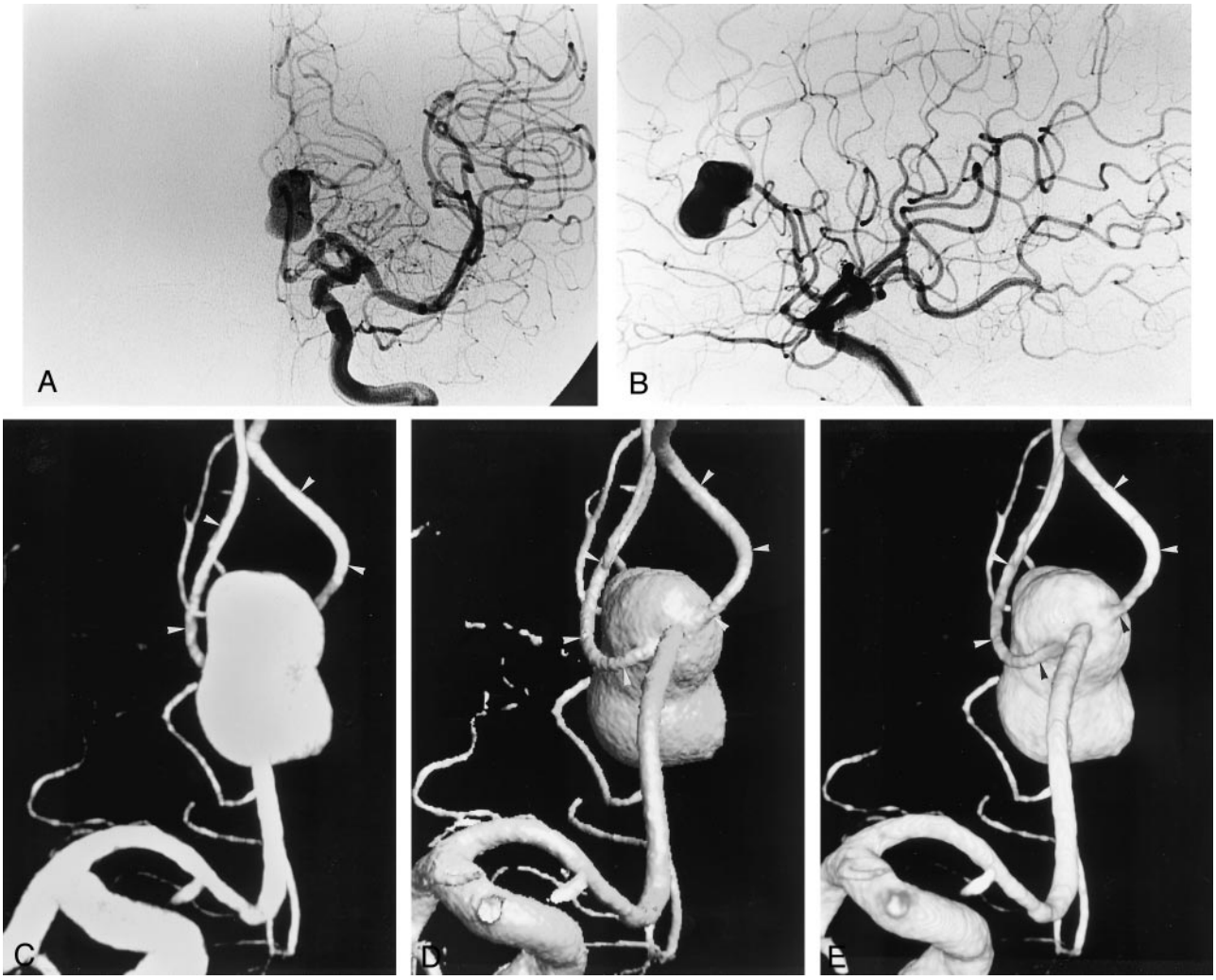

FIG 2. Left distal anterior cerebral artery aneurysm in a 69-year-old man.

A, Anteroposterior and *B*, lateral 2D DSA images of the left internal carotid artery depict a 19-mm aneurysm at the distal anterior cerebral artery. However, the relationship between the aneurysm and the adjacent arteries is not clearly demonstrated on this 2D DSA image and the rotational DA image (not shown). Regarding the relationship on rotational DA image, two observers ranked it as ambiguous visualization.

C–E, Three-dimensional DA images from behind depict a distal anterior cerebral aneurysm. MIP 3D image (*C*) does not demonstrate the relationship between the aneurysm and the two adjacent arteries (arrowheads) deriving from the aneurysm because of superimposition of the aneurysm and the arteries; the two observers classified this aneurysm as insufficient visualization on delineation of shape and relationship. The SSD (*D*) and volume-rendering (*E*) 3D images clearly show the shape and relationship (arrowheads), which were ranked as sufficient visualization by the two observers. Neurosurgeons chose to performed surgery on the basis of this additional information, and the relationship was confirmed during surgery.

be obtained with the 3D images. The number of projections of 2D DSA could be reduced when evaluating intracranial aneurysms with the 3D angiograms. Recently, Abe et al (15) reported that 3D DSA could reduce the number of exposures in interventional procedures for ruptured aneurysms. However, it is not fully understood whether 3D angiograms reduce the examination time, volume of contrast material administrated, and radiation dose to patients. Further investigation needs to be performed in this matter. In our study, total examination time per person seemed to be shorter than that of previous angiographic study because only one biplane study, a lateral and anteroposterior view, for a selected artery was usually performed for 2D DSA. Since 2D DSA provides precise information about intracranial hemodynamics and all the cerebral vasculatures, including the venous structures, it cannot be omitted at the present time.

Three-dimensional DA has several limitations for assessing aneurysms before treatment. In comparison with 2D DSA, 3D DA may not always depict perforators of the parent artery. This could be due to the poorer spatial resolution of 3D DA than that of 2D DSA. Second, 3D DA does not provide precise information about intracranial hemodynamics and all the cerebral vasculature, including the venous structures. In surgery, the preoperative information about the venous structures may be an important factor in determining the surgical approach. Third, the 3D algorithms provide angiogram-like images, but the lower opacified features of the vessels may be lost, resulting

in a loss of visibility of small vessels. Fourth, 3D DA requires relatively large amounts of contrast material. We usually administered 24–32 mL of contrast material per acquisition. If the rotation speed of the C-arm becomes faster, the amount of contrast material can be reduced.

The limitations of 3D DA compared with 3D CT angiography are as follows. First, 3D DA did not demonstrate the contralateral A1 segment of the anterior cerebral artery in anterior communicating aneurysms. Carotid angiograms with manual compression of the carotid artery during contrast material injection are necessary in the preoperative evaluation of anterior communicating aneurysms. Second, information about the relationship between aneurysm and bony structures, calcification of the aneurysm wall, and thrombus within the aneurysm is missing with 3D DA. The information may be valuable in deciding treatment, such as aneurysm clipping or endovascular embolization (16, 17).

There are some limitations in this study. First, a direct comparison between 2D DSA and 3D DA was not performed. Since previous studies (1–5) have demonstrated the increased value of 3D DSA to 2D DSA, it was considered that only two or three 2D DSA projections were enough for aneurysm assessment when performing 3D DA examinations. Second, we did not compare 3D DA with 3D DSA with regard to image quality in this study. Further investigation must be performed to determine whether 3D DA is superior to 3D DSA in the evaluation of intracranial vascular lesions. Third, the results were acquired from a small group of patients, and few aneurysms in the posterior fossa were present in this study. However, the results warrant further study by using a larger group of patients to investigate the value of 3D DA in assessing intracranial aneurysms.

Conclusion

Three-dimensional DA with unsubtracted images often provided additional information to that of rotational DA in the pretreatment evaluation of intracranial aneurysms and provided useful information to treatment decisions in some aneurysms. Among the various display techniques, the volume-rendering technique provided the most sufficient information. It is considered that this 3D DA technique has several advantages over the 3D DSA technique: no probability of misregistration associated with the subtraction technique, less chance of motion artifacts, and less ionizing radiation. Further investigation must be performed to determine which technique is more suitable in the evaluation of intracranial aneurysms, 3D DA or 3D DSA.

References

1. Schueler BA, Sen A, Hsiung H-H, Latchaw RE, Hu X. **Three-dimensional vascular reconstruction with a clinical x-ray angiography system.** *Acad Radiol* 1997;4:693–699
2. Heautot JF, Chabert E, Gandon Y, et al. **Analysis of cerebrovascular diseases by a new 3-dimensional computerised x-ray angiography system.** *Neuroradiology* 1998;40:203–209
3. Bidaut LM, Laurent C, Piotin M, et al. **Second-generation three-dimensional reconstruction for rotational three-dimensional angiography**. *Acad Radiol* 1998;5:836–849
4. Missler U, Hundt C, Wiesmann M, Mayer T, Brückmann H. **Three-dimensional reconstructed rotational digital subtraction angiography in planning treatment of intracranial aneurysms.** *Eur Radiol* 2000;10:564–568
5. Anxionnat R, Bracard S, Ducrocq X, et al. **Intracranial aneurysms: clinical value of 3D digital subtraction angiography in the therapeutic decision and endovascular treatment.** *Radiology* 2001;218:799–808
6. Grass M, Koppe R, Klotz E, et al. **Three-dimensional reconstruction of high contrast objects using C-arm image intensifier projection data.** *Comput Med Imaging Graph* 1999;23:311–321
7. Van den Berg JC, Overtoom TThC, de Valois JC, Moll FL. **Using three-dimensional rotational angiography for sizing of covered stents.** *AJR Am J Roentgenol* 2002;178:149–152
8. Fleiss JL, ed. *Statistical Methods for Rates and Proportions.* 2nd ed. New York: Wiley, 1981;212.
9. Schumacher M, Kutluk K, Ott D. **Digital rotational radiography in neuroradiology**. *AJNR Am J Neuroradiol* 1989;10:644–649.
10. Hoff DJ, Wallace MC, terBrugge KG, Gentili F. **Rotational angiography assessment of cerebral aneurysms** *AJNR Am J Neuroradiol* 1994;15:1945–1948.
11. Tu RK, Cohen WA, Maravilla KR, et al. **Digital subtraction rotational angiography for aneurysms of the intracranial anterior circulation: injection method and optimization**. *AJNR Am J Neuroradiol* 1996;17:1127–1136
12. Kuszyk BS, Heath DG, Ney DR, et al. **CT angiography with volume rendering: imaging findings.** *AJR Am J Roentgenol* 1995;165:1579–1580
13. Johnson PT, Heath DG, Kuszyk BS, Fishman EK. **CT angiography with volume-rendering: advantages and application in splanchnic vascular imaging.** *Radiology* 1996;200:564–568
14. Setton A, Davis AJ, Bose A, Nelson PK, Berenstein A. **Angiography of cerebral aneurysms.** *Neuroimag Clin North Am* 1996;6:705–738
15. Abe T, Hirohata M, Tanaka N, et al. **Clinical benefits of rotational 3D angiography in endovascular treatment of ruptured cerebral aneurysm.** *AJNR Am J Neuroradiol* 2002;23:686–688
16. Aoki S, Sasaki Y, Machida T, Ohkubo T, Minami M, Sasaki Y. **Cerebral aneurysm: detection and delineation using 3D CT angiography.** *AJNR Am J Neuroradiol* 1992;13:1115–1120
17. Ogawa T, Okudera T, Noguchi K, et al. **Cerebral aneurysms: evaluation with three-dimensional CT angiography.** *AJNR Am J Neuroradiol* 1996;17:447–454